International Journal of Greenhouse Gas Control 95 (2020) 102952

Contents lists available at ScienceDirect

International Journal of Greenhouse Gas Control

journal homepage: www.elsevier.com/locate/ijggc

Absorption of carbon dioxide in mixtures of N-methyl-2-pyrrolidone and 2-amino-2-methyl-1-propanol

Hanna K. Karlsson, Meher G. Sanku, Helena Svensson*

Dept. of Chemical Engineering, Lund University, PO Box 124, SE-221 00, Lund, Sweden

ARTICLE INFO

Keywords:
CO_2
Solubility
Heat of absorption
NMP
AMP
Henry's constant

ABSTRACT

It has been suggested that non-aqueous solvents containing amines may provide alternatives to aqueous alkanolamine solvents due to the potentially lower energy requirement for the regeneration of the amine. This paper presents experimental data on the solubility of CO_2 and heat of absorption in the organic solvent N-methyl-2-pyrrolidone (NMP) and mixtures of 2-amino-2-methyl-1-propanol (AMP) in NMP. The solubility of CO_2 was found to be very low at temperatures above 70 °C, the temperature at which the AMP/NMP solvent can be regenerated. The solubility of CO_2 was higher at lower temperatures, particularly when precipitation of the AMP carbamate occurred. The heat of absorption in the AMP/NMP solvent decreased with increasing temperature, from approximately 90 kJ/mol CO_2 at 40 °C and low loadings, to approximately 40 kJ/mol CO_2 and 65 kJ/mol CO_2, at 88 °C and low loadings, for the 15 wt% and 25 wt% AMP in NMP solvents, respectively. The results obtained complement our previous studies, together providing comprehensive data on the vapor–liquid equilibrium and the heat of absorption of CO_2, which can be used to model the system.

1. Introduction

The removal of CO_2 from gas mixtures is an important industrial process, for example, in biogas upgrading, and in the production of synthesis gas and hydrogen. The technology used for CO_2 removal is also of interest for carbon capture and storage to reduce the CO_2 emission from power plants and other industrial facilities. The most common method of CO_2 removal is absorption in aqueous alkanolamines such as monoethanolamine (MEA), which is currently considered the most feasible option for CO_2 removal. However, its use has been limited, mainly due to the high operating cost, in part resulting from the high amount of energy required for absorbent regeneration (Zhang et al., 2019). The energy required for absorbent regeneration depends on the heat of reaction of the amine, the sensible heat needed in the stripper to increase the temperature of the solvent to the reboiler temperature, and the heat of vaporization required to vaporize part of the solvent (Meldon, 2011).

Current research is ongoing in investigating new amine systems with high cyclic capacities and fast reaction kinetics (Liu et al., 2019a, b), water-lean amine systems (Garcia et al., 2018; Pakzad et al., 2018; Yuan and Rochelle, 2018) and phase changing solvents (Barzagli et al., 2017; Ye et al., 2015; Zhou et al., 2017), with the possibility of a reduced energy requirement for regeneration. Non-aqueous solvents have also been suggested as a means of reducing the operating cost of the absorption process, as the temperature required for the regeneration of such systems is relatively low which reduces the heat needed for vaporization. Also, the heat capacity of the solvent is typically lower than that of water (Zhang et al., 2019).

One of the amines widely studied in non-aqueous solvents is the sterically hindered, primary amine 2-amino-2-methyl-1-propanol (AMP) (Barzagli et al., 2018, 2019; Barzagli et al., 2014; Zhang et al., 2019; Zheng et al., 2012, 2013). In non-aqueous solutions of AMP the reaction of CO_2 is directed towards the formation of carbamate or alcohol carbonate (Barzagli et al., 2019; Zhang et al., 2019), which can be regenerated at relatively low temperatures, 80 − 90 °C (Svensson and Karlsson, 2018; Zhang et al., 2019). The AMP carbamate has also been found to precipitate in non-aqueous solutions of 1-propanol, triethylene glycol dimethyl ether and N-methyl-2-pyrrolidone (NMP) (Barzagli et al., 2013; Svensson et al., 2014b). A reaction mechanism has been suggested for the absorption of CO_2 in a non-aqueous solution of AMP and is listed below. Reaction 1 describes the dissolution of CO_2 in the solvent, and Reaction 2 describes the formation of the AMP carbamate (g denotes the gas phase, sol denotes in solution, and s denotes the solid phase).

$$CO_2\ (g) \leftrightarrow CO_2\ (sol) \quad (R1)$$

* Corresponding author.
E-mail address: helena.svensson@chemeng.lth.se (H. Svensson).

https://doi.org/10.1016/j.ijggc.2019.102952
Received 24 June 2019; Received in revised form 19 December 2019; Accepted 26 December 2019

CO_2 (sol) + 2 RNH_2 (sol) ↔ RNH_3^+ (sol) + $RNHCOO^-$ (sol) (R2)

The AMP carbamate can precipitate in the solvent, according to Reaction 3.

RNH_3^+ (sol) + $RNHCOO^-$ (sol) ↔ $RNH_3^+RNHCOO^-$ (s) (R3)

Additionally, if alcohol is used as a solvent, it can react with CO_2 in the presence of a base, such as AMP, to produce alkyl carbonates, according to Reaction 4 (Barzagli et al., 2019; Zhang et al., 2019).

CO_2 (sol) + RNH_2 (sol) + R'OH ↔ RNH_3^+ (sol) + $R'OCOO^-$ (sol) (R4)

Although non-aqueous AMP solvents have been widely studied in recent years (Barzagli et al., 2018, 2019; Barzagli et al., 2014, 2013; Svensson et al., 2014a, c; Zheng et al., 2012, 2013), little data are available in the literature on the solubility of CO_2 and the heat of absorption at higher temperatures (Svensson and Karlsson, 2018). To assess the performance of these systems, information regarding solubility at both absorption and desorption temperatures is needed. In addition, this data combined with data on the heat of absorption for these types of systems can provide important information regarding the reactions occurring at the different temperatures and help elucidate the mechanism of regeneration.

In this work we have studied the solubility and heat of absorption of CO_2 in pure NMP and solutions of 15 wt% AMP in NMP and 25 wt% AMP in NMP, at temperatures between 37 and 88 °C, where both absorption and regeneration conditions are represented. Henry's constant for CO_2 in NMP was determined from the solubility data for the investigated temperatures. In addition, parameters for a model describing the temperature dependency of Henry's constant were also fitted to experimental data. This study complements our previous studies (Svensson et al., 2014a; Svensson and Karlsson, 2018; Svensson et al., 2014c), together providing comprehensive data on vapor–liquid equilibrium and the heat of absorption. Such data are essential for the reliable assessment of the energy performance of the absorption process, and the development of thermodynamic models for biphasic non-aqueous solvents.

2. Materials and method

2.1. Materials

The chemicals used were NMP, AMP and CO_2. NMP, with a purity of 99.5 %, was purchased from Sigma Aldrich, and AMP, with a purity of 93–98 %, was purchased from Merck. The chemical structures of AMP and NMP are shown in Fig. 1. CO_2, with a purity of > 99.99 %, was purchased from AGA. All chemicals were used as received without further purification. The solutions of AMP and NMP were prepared by weight using a scale with an accuracy of 0.01 g for weights up to 1200 g.

2.2. Experimental method

The experimental method used has been previously described in Svensson et al. (2014a); (2014c), and therefore only a brief description of the method is given here. Experiments were performed using three solutions with different concentrations of amine (AMP) and organic solvent (NMP). The solutions used and a summary of the experimental conditions are given in Table 1.

All experiments were conducted with a true heat flow reaction calorimeter (CPA201 Chemical Process Analyzer from ChemiSens AB) with a reactor of glass and stainless steel with an effective volume of 250 cm^3. The experimental setup is illustrated in Fig. 2.

Prior to each experiment, approximately 100 g of solution was loaded in the reactor. Before each experimental run, the solution was degassed for 10 − 12 s by reducing the pressure in the reactor using a vacuum pump. The vapor pressure of amine and solvent in the gas phase of the reactor was assumed to be constant and equal to the total equilibrium pressure before the first addition of CO_2 to the reactor. All experiments were conducted at a constant temperature (see Table 1), and pure CO_2 was injected into the system via a Bronkhorst Hi-Tec mass flow controller, with an accuracy of ± 0.8 %. CO_2 was injected for approximately 10 s or until a set pressure was reached. The system was then allowed to reach equilibrium before CO_2 was again introduced into the reactor. An automation script was used to run the experiments, which seeks stability in true heat flow and pressure between each addition of CO_2. The maximum deviation in the true heat flow and pressure were required to be below ± 0.02 W and ± 0.005 bar, respectively, for a duration of 30 min, for the system to be considered to be at equilibrium.

Two to four independent experiments were performed at each temperature for each solution, and each experiment consisted of four to ten equilibrium points. The amount of CO_2 added to the reactor, the heat flow from the reactor, and the pressure in the reactor were logged continuously. The pressure was measured with an Omega pressure transducer with an accuracy of ± 1.0 %, and the accuracy of the temperature sensor was ± 2.7 K (at 100 °C). The uncertainties in the amount of absorbed CO_2 were evaluated and determined to be ± 2.1 % for the pure solvent, ± 1.0 % for the 15 wt% AMP/NMP mixture, and ± 0.8 % for the 25 wt% AMP/NMP mixture. The uncertainties in the differential heat of absorption were determined to be ± 7.0 % for the pure solvent, ± 2.5 % for 15 wt% AMP/NMP, and ± 2.0 % for 25 wt% AMP/NMP.

2.3. Evaluation of data

Henry's constant was determined for NMP at each temperature studied, using Eq. (1):

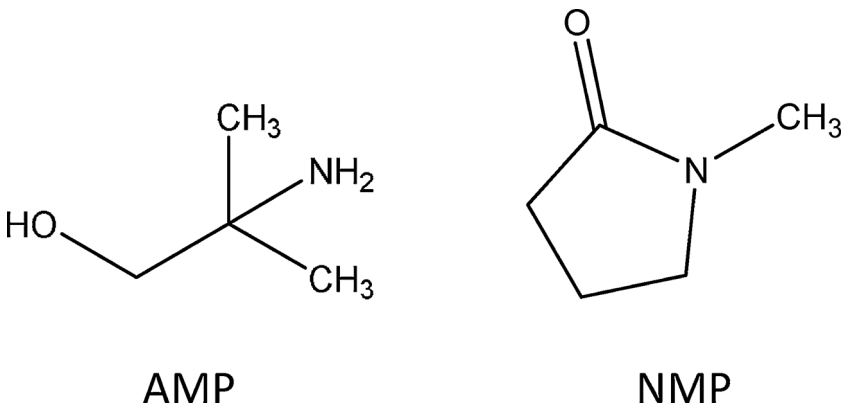

Fig. 1. Chemical structure of 2-amino-2-methyl-1-propanol (AMP) and organic solvent N-methyl-2-pyrrolidone (NMP).

Table 1
Composition of the solutions used in the present study, together with a summary of the temperatures at which the solubility of CO_2 and the heat of absorption were determined and the range of partial pressure of CO_2.

Solution	wt% NMP	wt% AMP	Solubility of CO_2	Heat of absorption	P_{CO2} (kPa)
1	100	0	37, 40, 60, 70, 80 and 88 °C	37, 40, 60, 70, 80 and 88 °C	17.4–386
2	85	15	60, 70 and 80 °C	40, 60, 70, 80 and 88 °C	2.49–353
3	75	25	60, 70 and 80 °C	40, 60, 70, 80 and 88 °C	1.23–342

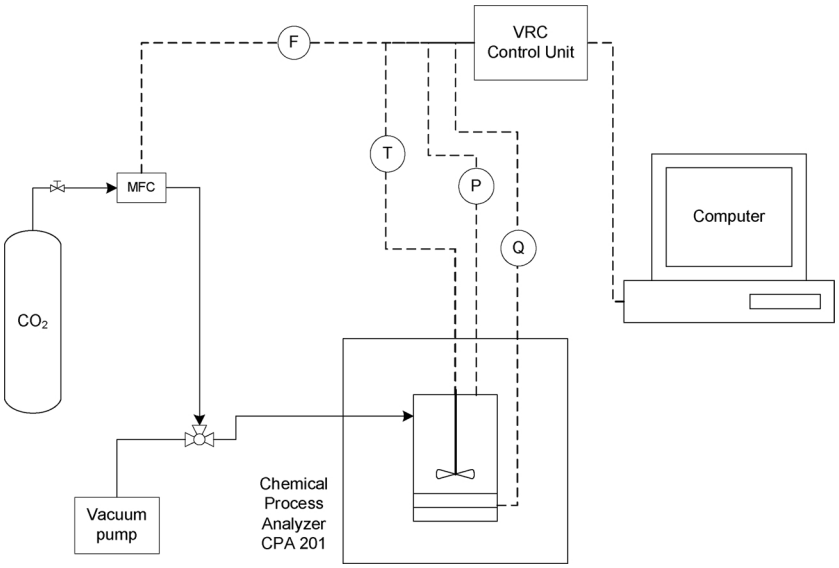

Fig. 2. Schematic of the experimental setup used in this study. MFC denotes the mass flow controller, F is the flow signal from the MFC, T is the temperature signal, P is the pressure signal and Q is the true heat flow signal logged. The VRC control unit controls the MFC and collects all signals during the experiment.

$$H_{CO_2} = \frac{P_{CO_2}}{x_{CO_2}} \tag{1}$$

where x_{CO_2} is the molar fraction of CO_2 in the solvent and P_{CO_2} is the partial pressure of CO_2 above the solvent. Linear fits to the equilibrium points were made for the experiments performed at each temperature, and the slope of the linear fits gives Henry's constant for the solvent at that temperature.

A model of the temperature dependency of Henry's constant was also derived according to Eq. (2):

$$\ln H(T) = \left[A + \frac{B}{T} + C\ln T + DT\right] \tag{2}$$

where Henry's constant, H, is expressed in Pa and temperature, T, in K The coefficients A, B, C, and D in Eq. (2), were determined using the solver tool in MS Excel™. The solver minimizes the objective function, given in Eq. (3), by iteratively varying the coefficients A, B, C, and D, and returns the values of the coefficients at which the objective function has a minimum.

$$f = \sqrt{\sum_{i=1}^{N} (P_{est} - P_{exp})^2} \tag{3}$$

N is the number of data points, P_{exp} is the partial pressure of CO_2 measured in the experiment, and P_{est} is the partial pressure of CO_2 estimated with the parameters in Eq. (2).

The mean squared error of the estimate (MSE) was determined using Eq. (4):

$$MSE = \frac{\left(\sum_{i=1}^{N}\left(\frac{P_{exp} - P_{est}}{P_{exp}}\right)^2\right)}{N-2} \tag{4}$$

The amount of CO_2 that was absorbed in the solution was calculated using to Eq. (5):

$$(CO_2)_{abs} = (CO_2)_{added} - \frac{P_{CO_2} V}{RT} \tag{5}$$

where V is the reactor head space volume over the amine solution, R is the molar gas constant, T is the temperature, and $(CO_2)_{added}$ is the amount of CO_2 added to the reactor.

The CO_2 loading of the amine solution was defined as the amount of CO_2 absorbed (moles) per mole of amine in the solution, according to Eq. (6). According to the proposed reaction mechanism, each mole of CO_2 reacts with two moles of amine. The CO_2 loading can exceed 0.5 mol CO_2/mole amine when physical absorption in the organic solvent also takes place.

$$\alpha = \frac{(CO_2)_{abs}}{(C_{AMP})_0} \tag{6}$$

$(C_{AMP})_0$ is the amount of amine (AMP) present in the system at the start of the experiment.

The heat of absorption ($-\Delta H_{abs}$) was estimated using Eq. (7), in terms of the heat produced in the reactor (, [kJ]) and the amount of CO_2 absorbed. Q was determined by integrating the true heat flow curve from one equilibrium point to the next. The energy required to heat the CO_2 gas stream entering the reactor, from ambient temperature to the reactor temperature, was also added to.

$$-\Delta H_{abs} = \frac{Q}{(CO_2)_{abs}} \tag{7}$$

The integral heat of absorption is determined by dividing the total amount of heat released by the total amount of CO_2 absorbed up to the considered equilibrium point. The differential heat of absorption is determined by dividing the heat released upon each addition of CO_2 by the amount of CO_2 absorbed with each addition.

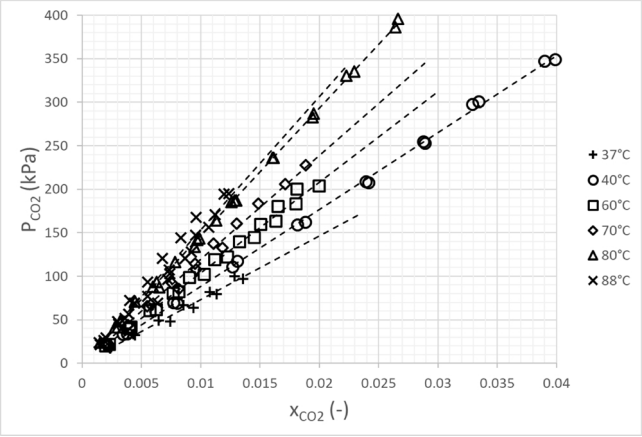

Fig. 3. Solubility of CO_2 in NMP at 37, 40, 60, 70, 80 and 88 °C. The linear fits used to determine Henry's constant are indicated by the dashed lines, some of which have been projected forward to improve visibility.

3. Results and discussion

3.1. Pure solvent

Henry's constant was determined for the pure solvent (NMP) at 37, 40, 60, 70, 80 and 88 °C. The solubility data for CO_2 in NMP are shown in Fig. 3, together with the linear fits used to determine Henry's constant (using Eq. (1)). The values obtained for Henry's constant are presented in Table 2.

The results show that Henry's constant increases with increasing temperature. The difference between the results at 80 °C and 88 °C was smaller than those between the other temperatures. The variation in the results obtained in the four experiments performed at 88 °C was greater than at the other temperatures; R^2 for the linear fit at 88 °C being 0.96, and $R^2 > 0.99$ for the other linear fits. The values of Henry's constant determined in this work are in good agreement with those reported in the literature, as can be seen from Table 2. However, most of the data reported in the literature were obtained at temperatures between 25 and 50 °C, while very few data have been reported at higher temperatures.

Table 2
Values of Henry's constant for CO_2 in NMP, at 37, 60, 70, 80 and 88 °C. Values obtained from the literature, used to determine the model describing the temperature dependence of Henry's constant, at 25, 40, 50 and 75 °C, are also included.

Temperature (°C)	H (MPa)	Reference
25	6.97	Svensson et al. (2014b)
	6.69	Rivas and Prausnitz (1979)
	6.94	Murrieta-Guevara and Trejo Rodriguez (1984)
	6.56	Melzer et al. (1989)
	6.38	Murrieta-Guevara et al. (1988)
	6.98	Sweeney (1984)
37	7.32	This work
40	8.85	Karlsson and Svensson (2018)
	8.04*	Kassim et al. (1988)
50	10.5	Svensson et al. (2014b)
	10.0	Rivas and Prausnitz (1979)
	10.2	Murrieta-Guevara and Trejo Rodriguez (1984)
	10.1	Murrieta-Guevara et al. (1988)
	11.1	Sweeney (1984)
	9.56*	Kassim et al. (1988)
60	10.4	This work
	10.4*	Kassim et al. (1988)
70	11.9	This work
75	13.9	Rivas and Prausnitz (1979)
80	14.7	This work
88	15.3	This work

* Calculated from data reported by Kassim et al. (1988).

Table 3
Values of the coefficients of the model describing the temperature dependency of Henry's constant for CO_2 in NMP, according to Eq. (2).

A	B	C	D
94.05	−369.3	−16.57	0.05849

The solubility data determined in this work were used together with data from the literature (ASPEN, 2017; Kassim et al., 1988; Melzer et al., 1989; Murrieta-Guevara et al., 1988; Murrieta-Guevara and Trejo Rodriguez, 1984; Svensson et al., 2014b), where pressure vs. mole fraction of CO_2 were available, to obtain a model of the temperature dependency of Henry's constant, according to Eq. (2). The temperature was limited to the range 25–90 °C, and the partial pressures of CO_2 was limited to values below 0.8 MPa, which corresponds to a maximum molar fraction of CO_2 of 0.094.

Regression in Excel, minimizing the objective function given in Eq. (3), led to the results presented in Table 3, where the values of the coefficients used in Eq. (2) are given. The value of MSE obtained using Eq. (4) was 0.013.

A parity plot, where the values of Henry's constant calculated using the derived model are compared to the values given in Table 2, is shown in Fig. 4. The predicted values, calculated with the derived model, gives the same value for the same temperature, in contrast to the experimentally determined values which can differ for the same temperature, see Table 2. This can be seen in Fig. 4 where calculated values appear on the same line at temperatures of 25, 40 and 50 °C, corresponding to values of Henry's constant of 7.6, 8.6 and 9.5 MPa respectively. It can be seen that there is good agreement between the experimentally determined values of Henry's constant and those calculated using the model, at all temperatures.

The heat of absorption of CO_2 in pure NMP was very similar at the temperatures studied, as can be seen in Fig. 5 and Table 4. The effect of temperature on the heat of absorption is thus small, as observed in our previous study (Svensson et al., 2014c). The average heat of absorption over all temperatures, 17.8 kJ/mol CO_2, is very similar to that previously reported at 25 and 50 °C, 17.3 kJ/mol CO_2 (Svensson et al., 2014c), and with values reported in the literature, 14.78 kJ/mol CO_2

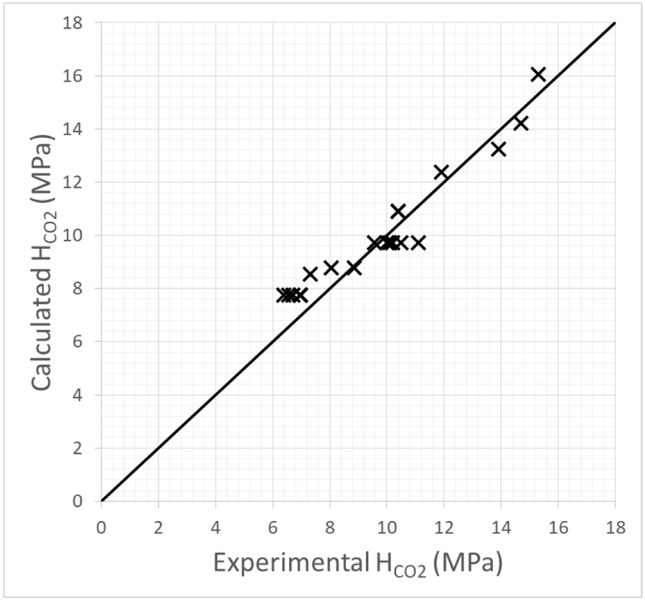

Fig. 4. Parity plot comparing the values of Henry's constant calculated using the model derived in this work with experimentally determined values for temperatures between 25 and 88 °C.

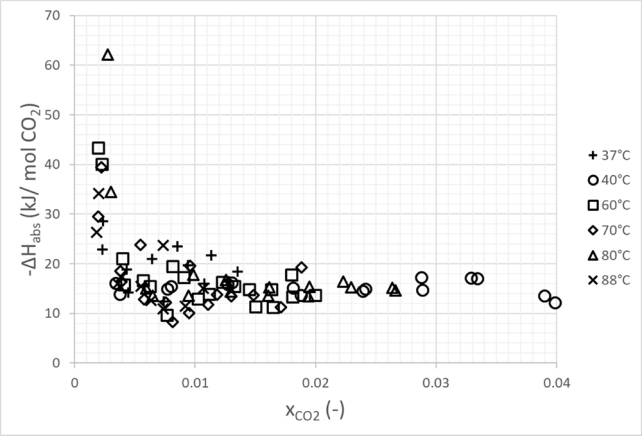

Fig. 5. Differential heat of absorption as a function of mole fraction of CO_2 in NMP at 37, 40, 60, 70, 80 and 88 °C.

Table 4
Experimentally determined differential heat of absorption of CO_2 in pure solvent, NMP, averaged for each temperature, at 37, 40, 60, 70, 80 and 88 °C, and the average value over all temperatures.

Temperature (°C)	-ΔH_{abs} (kJ/mol CO_2)
37	19.4
40	15.1
60	17.7
70	17.1
80	19.2
88	18.3
Average	17.8

(Melzer et al., 1989). These values are also in the same range as reported in literature for other solvents, for example 11.40 kJ/mol CO_2 (Sciamanna and Lynn, 1988) and 16.9 kJ/mol CO_2 (Svensson et al., 2014c) for triethylene glycol dimethylether, and 14.3 kJ/mol CO_2 for dimethyl sulfoxide (Karlsson et al., 2019).

As can be seen from Fig. 5, the differential heat of absorption determined in this work was higher for the first injection of CO_2. This was also observed at 25 and 50 °C in our previous study (Svensson et al., 2014c), although the values are higher in the present study. This phenomenon was only observed at mole fractions of CO_2 below 0.003.

3.2. Solvent mixtures

The results regarding the solubility of CO_2 in mixtures of 15 wt% AMP in NMP and 25 wt% AMP in NMP are given in Figs. 6 and 7, respectively, showing how the solubility is affected by temperature. Data from our previous studies, at 25, 40, 50 and 88 °C, are also included (Svensson et al., 2014a; Svensson and Karlsson, 2018).

For the solvent mixture containing 15 wt% AMP in NMP, precipitation of AMP carbamate was only observed at 25 and 40 °C (Fig. 6). At 40 °C, precipitation occurred at CO_2 loadings above 0.5 mol CO_2/mol AMP, while at 25 °C precipitation occurred already at a CO_2 loading of approximately 0.35 mol CO_2/mol AMP.

The same behavior was observed in the 25 wt% AMP/NMP mixture (Fig. 7) and the 15 wt% AMP/NMP mixture. The solubility of CO_2 in 25 wt% AMP/NMP was somewhat higher at lower temperatures, 25 – 50 °C, than in 15 wt% AMP/NMP. This is largely due to the fact that precipitation occurs at these temperatures, and at a lower CO_2 loading of 0.2-0.3 mol CO_2/mol AMP. It is thus possible to achieve a higher CO_2 loading in the 25 wt% AMP/NMP solvent, 0.3-0.45 mol CO_2/mol AMP, even at a relatively low partial pressure of CO_2, 10 – 20 kPa. The solubility of CO_2 at higher temperatures, 70 – 88 °C,

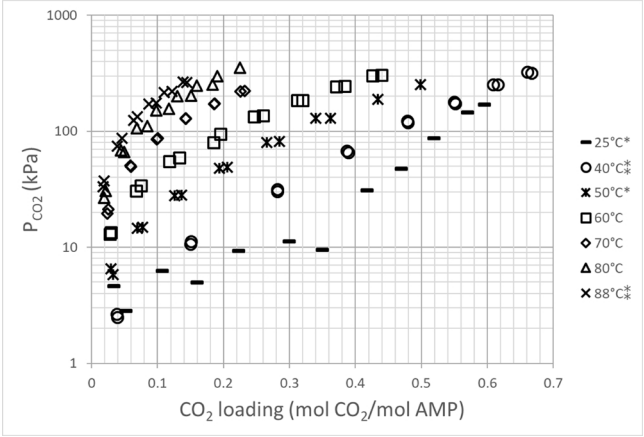

Fig. 6. Solubility of CO_2 in 15 wt% AMP in NMP at 60, 70 and 80 °C. Data from our previous studies are also included, indicated by an asterisk (Svensson et al., 2014a) and a double asterisk (Svensson and Karlsson, 2018) in the legend.

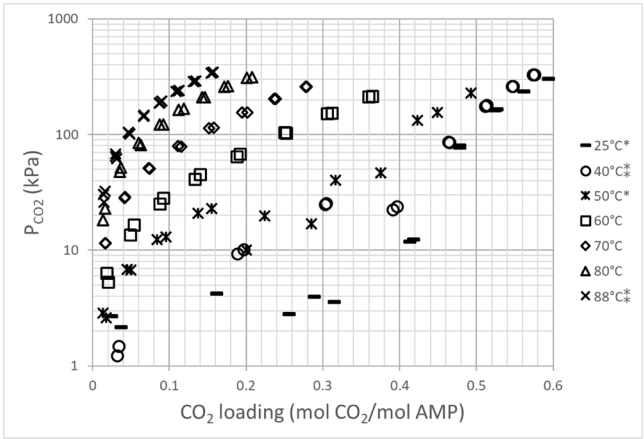

Fig. 7. Solubility of CO_2 in 25 wt% AMP/NMP at 60, 70 and 80 °C. Data from our previous studies are also included, indicated by an asterisk (Svensson et al., 2014a) and a double asterisk (Svensson and Karlsson, 2018) in the legend.

was significantly lower, and very similar to that obtained in 15 wt% AMP/NMP.

Based on the solubility data obtained for the AMP/NMP system in this, and our previous studies (Svensson et al., 2014a; Svensson and Karlsson, 2018), temperatures of 25 – 50 °C can be said to represent absorption conditions, while temperatures of 70 – 88 °C represent desorption conditions for both 15 and 25 wt% AMP/NMP solvent mixture. The very low CO_2 solubility at temperatures of 70 – 88 °C indicates that very low lean loadings can be achieved in the AMP/NMP system, even at low regeneration temperatures, which would make it possible to use low-grade heat, such as excess heat in industry, for regeneration of the solution. The low solubility of CO_2 at absorption conditions and low partial pressures of CO_2 for the 15 wt% AMP/NMP mixture, compared to the 25 wt% AMP/NMP mixture, indicate that a higher amine concentration is preferable to achieve a significantly high rich loading. As the regeneration temperature is so low for the AMP/NMP solutions, the temperature in the absorption column would have to be kept in the range conducive to absorption during the operation of a full-sized plant. It is thus likely that intercooling of the solvent will be necessary to reduce the risk of regeneration occurring in the absorption column, as the temperature of the solvent rises due to the of the heat of absorption released as the CO_2 reacts with AMP.

Fig. 8 presents data obtained in the present study, together with data from the literature for various aqueous and non-aqueous systems at various temperatures. Fig. 8**a)** shows data obtained in the present

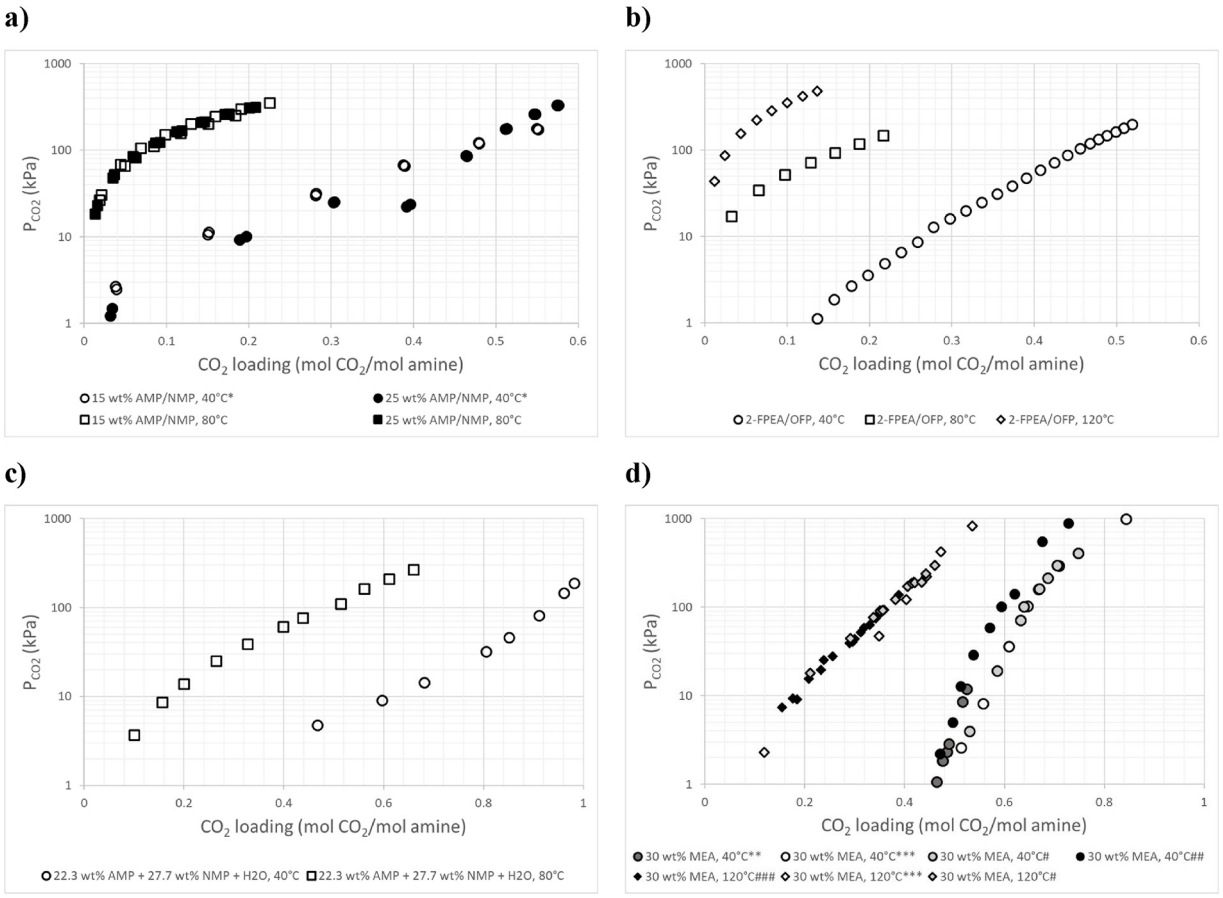

Fig. 8. Data on the solubility of CO_2 in various aqueous and non-aqueous systems. **a)** In AMP/NMP solutions at 40 °C and 80 °C from present study and our previous study (*(Svensson and Karlsson, 2018)), **b)** in 2-FPEA/OFP (Mobley et al., 2017), **c)** in AMP/NMP/H_2O solutions (Pakzad et al., 2018), and **d)** in aqueous 30 wt% MEA (**(Aronu et al., 2011), ***(Jou et al., 1995), #(Tong et al., 2012), ##(Shen and Li, 1992), ###(Ma'mun et al., 2005)). ○ 40 °C, □ 80 °C and ◊ 120 °C.

study for 15 and 25 wt% AMP in NMP, at 40 and 80 °C. Fig. 8**b)** shows data for a non-aqueous solvent, 2-fluorophenethylamine in 2,2′,3,3′,4,4′,5,5′-octafluoropentanol (2-FPEA/OFP), at 40, 80 and 120 °C (Mobley et al., 2017). Fig. 8**c)** shows data for an aqueous solution containing AMP and NMP, at 40 and 80 °C (Pakzad et al., 2018). Fig. 8**d)** shows data for aqueous 30 wt% MEA, at 40 and 120 °C (Aronu et al., 2011; Jou et al., 1995; Ma'mun et al., 2005; Shen and Li, 1992; Tong et al., 2012).

The results from the present study, shown in Fig. 8**a)**, show that the solubility of CO_2 is very similar for both the 15 and 25 wt% AMP in NMP solution, at 80 °C. This is likely due to the fact that at this temperature there is little reaction between CO_2 and AMP occurring, which is also indicated by the fact that the solubility of CO_2 is very low. As can be seen from Fig. 8**a)** and **b)**, the solubility of CO_2 is similar in the AMP/NMP and the 2-FPEA/OFP systems at lower temperatures. The solubility of CO_2 at 80 °C is low for both systems, although the solubility in the 2-FPEA/OFP solution is not as low as in the AMP/NMP solutions until 120 °C. Overall, the solubility of CO_2 in the non-aqueous solutions (Fig. 8**a)** and **b)**) is lower at partial pressures around 10 kPa, than in the aqueous solutions shown in Fig. 8**c)** and **d)**. For instance, the solubility of CO_2 in the non-aqueous solutions at 40 °C is limited to loadings below 0.3 at low partial pressures of CO_2 (5–15 kPa) compared to the solubility in aqueous 30 wt% MEA, where a CO_2 loading of approximately 0.53 can be achieved, as seen in Fig. 8**d)**. However, the solubility of CO_2 in the AMP/NMP solvent at 80 °C is very low, 0.01-0.06 mol CO_2/mol AMP, at partial pressures of CO_2 of 10 − 100 kPa. This can be compared to the solubility in aqueous MEA, which has been reported to be 0.2 at 120 °C at a partial pressure of 10 kPa (Aronu et al., 2014; Knuutila and Nannestad, 2017). The behavior of the AMP/NMP/H_2O solution, shown in Fig. 8**c)**, is similar to the aqueous solution containing 30 wt% MEA, at a CO_2 partial pressure of 10 kPa, but differs somewhat at higher partial pressures of CO_2. The CO_2 solubility in the AMP/NMP/H_2O solution at 100 kPa, is higher at both 40 and 80 °C, than in 30 wt% MEA at 40 and 120 °C. If the solubility at 40 °C represents absorption conditions, and the solubility at 80 or 120 °C represents regeneration conditions, the difference between rich and lean loading that can be achieved for the solutions included in Fig. 8 is comparable, being approximately 0.3 mol CO_2/mol amine. A lower regeneration temperature is beneficial for the CO_2 removal process, as this would reduce both the sensible heat and the heat of vaporization required for regeneration.

The heat of absorption in 15 wt% AMP/NMP and 25 wt% AMP/NMP is given in Figs. 9 and 10, respectively. Data from our previous study at 25 and 50 °C (Svensson et al., 2014c) are also included to show how the heat of absorption is affected by temperature. The heat of absorption at 25 − 50 °C for the solvent mixtures containing 15 and 25 wt% AMP in NMP is shown in Figs. 9**a)** and 10 **a)**, and is about 90 kJ/mol CO_2 prior to the precipitation of AMP carbamate. When precipitation starts, the heat of absorption increases significantly, to values of about 170 − 220 kJ/mol CO_2. This is due to the supersaturation of the solution prior to precipitation, causing a large amount of AMP carbamate to precipitate at the same time. After these initial high values at the onset of precipitation, the heat of absorption is approximately 125 kJ/mol CO_2, and then decreases at higher loadings. At loadings above 0.5 mol CO_2/mol AMP, the heat of absorption approaches that in pure NMP, indicating that physical absorption dominates in this region. This is in agreement with the proposed reaction mechanism, where the maximum loading due to chemical absorption is

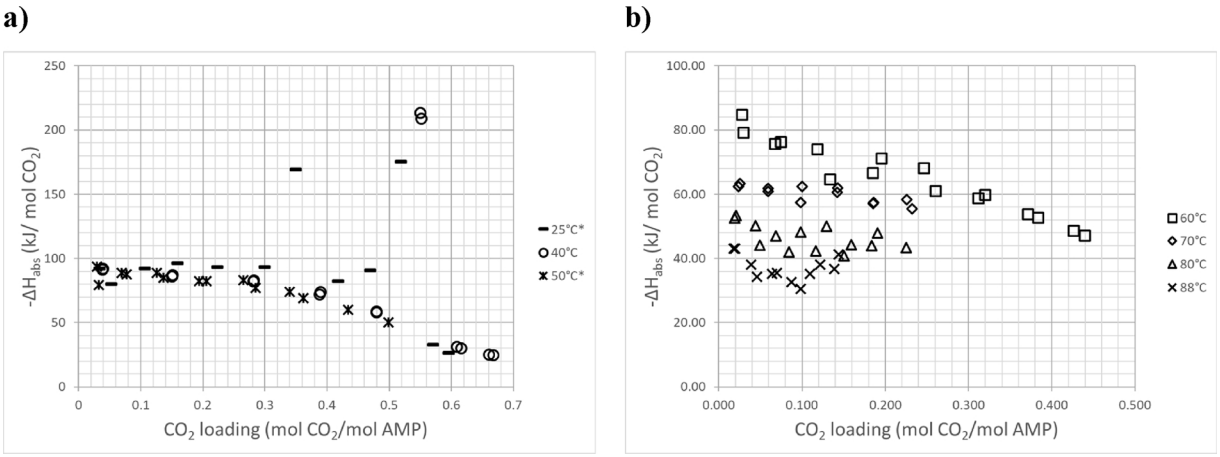

Fig. 9. Differential heat of absorption as a function of CO_2 loading in 15 wt% AMP/NMP at **a)** 25, 40 and 50 °C, and **b)** 60, 70, 80 and 88 °C. Data at 25 and 50 °C, indicated by an asterisk in the legend, are from our previous study (Svensson et al., 2014c).

limited to 0.5 mol CO_2/mol AMP.

At higher temperatures, 60 – 88 °C, Figs. 9**b)** and 10 **b)**, the heat of absorption can be seen to decrease as the temperature increases. This behavior is in contrast to that reported for aqueous 30 wt% MEA (Kim et al., 2014; Kim and Svendsen, 2007; Mobley et al., 2017), where the heat of absorption was reported to increase with temperature. However, a decrease in heat of absorption as temperature increases has also been reported for other non-aqueous solvents (Mobley et al., 2017). One of the data points at 80 °C, corresponding to a CO_2 loading of 0.11 mol CO_2/mol AMP and a heat of absorption of 93.9 kJ/mol CO_2 in Fig. 10**b)** is considered an outlier resulting from an anomaly in the registration of the MFC signal. Each injection of CO_2 had a duration of 12 s, but for this data point the amount of CO_2 injected (calculated from the MFC signal) was 25 % lower than for all other injections, leading to a higher heat of absorption (according to Eq. 7). This anomaly was only observed for this injection.

Mobley et al. (2017) reported that the heat of absorption was lower at higher temperatures in their hydrophobic non-aqueous solvent 2-FPEA/OFP. The 2-FPEA/OFP system also captures CO_2 in the form of a 2-FPEA carbamate, similarly to the AMP/NMP system. A comparison of the heat of absorption in the 2-FPEA/OFP and AMP/NMP mixtures is shown in Fig. 11. Only data points obtained prior to precipitation are included for the AMP/NMP mixtures at 40 °C, and the outlier for 25 wt % AMP/NMP at 80 °C, discussed above, is not included, in the figure. The heat of absorption is similar for the 2-FPEA/OFP and AMP/NMP solutions at 40 °C, but differs somewhat at higher temperatures. The

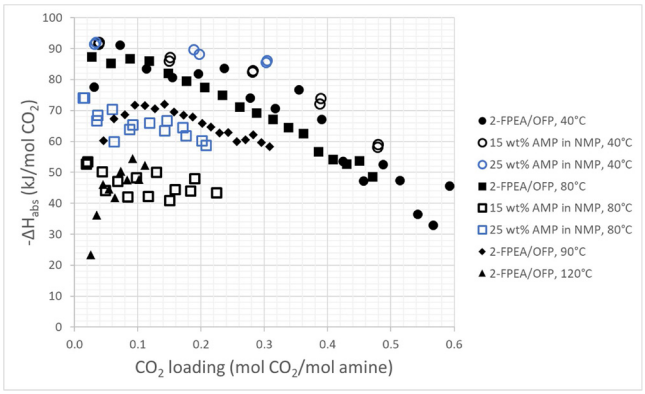

Fig. 11. Differential heat of absorption as a function of CO_2 loading for 2-FPEA/OFP at 40, 80, 90, and 120 °C (Mobley et al., 2017), and for 15 wt% AMP/NMP and 25 wt% AMP/NMP mixtures at 40 and 80 °C. Data points obtained prior to precipitation are included for AMP/NMP mixtures at 40 °C, and the outlier for 25 wt% AMP/NMP at 80 °C has been excluded.

heat of absorption in 25 wt% AMP/NMP at 80 °C is close to the value obtained for 2-FPEA/OFP at 90 °C, while the value in 15 wt% AMP/NMP at 80 °C is closer to that obtained for 2-FPEA/OFP at 120 °C. However, the general trend of decreasing heat of absorption with increasing temperature is the same for both solvents.

We suggest that the decrease in the heat of absorption is due to a

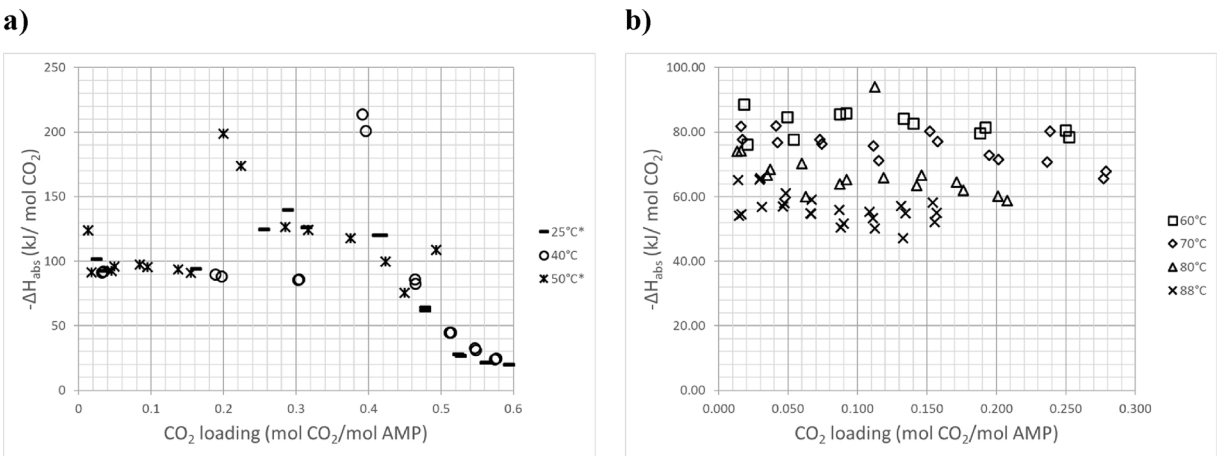

Fig. 10. Differential heat of absorption as a function of CO_2 loading in 25 wt% AMP/NMP at **a)** 25, 40 and 50 °C, and **b)** 60, 70, 80, and 88 °C. Data at 25 and 50 °C, indicated an asterisk in the legend, are from our previous study (Svensson et al., 2014c).

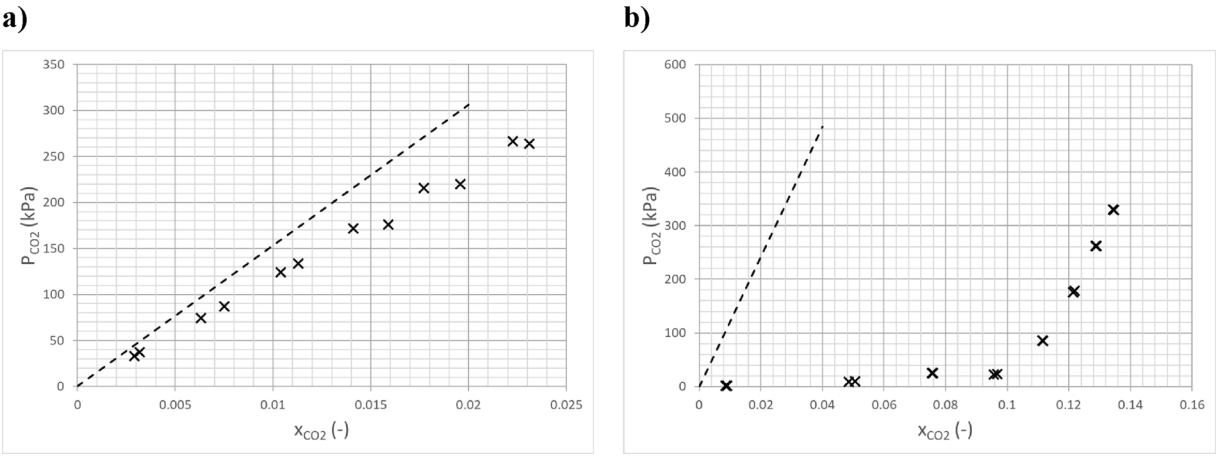

Fig. 12. Solubility of CO_2 in pure NMP and in a 15 wt% AMP in NMP mixture at **a)** 88 °C and **b)** 40 °C. The dashed lines show the physical solubility of CO_2 in **a)** pure NMP or **b)** 15 wt% AMP in NMP estimated using the N_2O analogy (Karlsson and Svensson, 2018), the data points show the measured solubility of CO_2 in 15 wt% AMP in NMP.

larger proportion of the absorbed CO_2 being physically absorbed at elevated temperatures, rather than reacting with AMP. Reactions 2 and 3 would thus be displaced to the left at higher temperatures. This theory was investigated by comparing the amount of CO_2 absorbed at 88 °C in the 15 wt% AMP/NMP solution to the amount that would be absorbed at the same temperature in pure NMP, as shown in Fig. 12**a)**. The amount of CO_2 that would be physically absorbed in a solution of AMP and NMP will differ slightly from a pure solution of NMP. The difference between Henry's constant in pure NMP and a 15 wt% AMP in NMP solution at 40 °C, estimated using the N_2O analogy (Karlsson and Svensson, 2018), is approximately 12 %. However, no estimates of Henry's constant in this mixture at 88 °C have been reported in the literature. For this reason, the physical solubility of CO_2 in the 15 wt% AMP/NMP solution was approximated with that of pure NMP.

The fraction of the absorbed amount of CO_2 that would be physically absorbed in pure NMP at 88 °C was determined to be 76 %. In a solution of AMP/NMP, this fraction would probably be slightly lower. If the remaining 24 % of absorbed CO_2 in the AMP/NMP solution reacts with AMP, the resulting heat of absorption can be estimated. A weighted average can be calculated if the heat of absorption for physical absorption in the solution (Reaction 1) and the heat of absorption for carbamate formation (Reactions 1 and 2) are known. The heat contribution from physical absorption was estimated using the average value of the heat of absorption obtained in pure NMP (17.8 kJ/mol CO_2), given in Table 3. The heat contribution from formation of the carbamate was estimated by the average heat of absorption at 25 – 50 °C prior to precipitation (88.6 kJ/mol CO_2), representing conditions where carbamate formation occurs. Using these values, the heat of absorption using a weighted average was found to be 34.8 kJ/mol CO_2, which is in close agreement with the average measured heat of absorption of 37.0 kJ/mol CO_2.

The amount of CO_2 absorbed at 40 °C was compared with that expected to be physically absorbed in the AMP in NMP solution using Henry's constant for the solution, estimated using the N_2O analogy (Karlsson and Svensson, 2018), as shown in Fig. 12**b)**. It is evident from the solubility data that the amount of physically absorbed CO_2 is considerably lower than the amount of CO_2 that reacts with AMP, at 40 °C.

4. Conclusions

The solubility of CO_2 and heat of absorption was measured and presented in this study for pure NMP and solutions of 15 wt% and 25 wt % AMP in NMP.

The solubility of CO_2 in AMP/NMP solutions is overall lower than in aqueous 30 wt% MEA, under both absorption and regeneration conditions. The solubility of CO_2 increases at partial pressures above 20 kPa, especially when precipitation of the carbamate occurs, making the AMP/NMP solution more suitable for CO_2 removal from gas mixtures with a higher partial pressure of CO_2, for example, in industrial applications and in biogas upgrading. The AMP/NMP solution can be regenerated at low temperatures, 70 – 90 °C, as the solubility of CO_2 is very low at these temperatures, and hence a low lean loading can be achieved during regeneration.

The results of this study showed that the heat of absorption of the AMP/NMP solutions decreases as the temperature increases, in contrast to aqueous solutions of MEA. This could be due to a larger fraction of the absorbed CO_2 being only physically absorbed, and not reacting with AMP. As the solubility of CO_2 is significantly higher in NMP than in water, this would probably have a greater effect on the measured heat of absorption in non-aqueous solutions at higher temperatures. To investigate this behavior further, quantitative *in situ* NMR spectroscopy could be used to determine the relative amounts of physically absorbed and reacted CO_2, and the products formed in AMP/NMP solutions at higher temperatures.

CRediT authorship contribution statement

Hanna K. Karlsson: Formal analysis, Investigation, Methodology, Validation, Writing - review & editing, Writing - original draft. **Meher G. Sanku:** Formal analysis, Investigation, Methodology, Validation, Writing - review & editing, Writing - original draft. **Helena Svensson:** Conceptualization, Formal analysis, Funding acquisition, Investigation, Methodology, Project administration, Supervision, Validation, Writing - review & editing, Writing - original draft.

Declaration of Competing Interest

The authors declare that they have no known competing financial interests or personal relationships that could have appeared to influence the work reported in this paper.

Acknowledgement

The Swedish Energy Agency is gratefully acknowledged for financial support through project 40532-1.

Appendix A. Supplementary data

Supplementary material related to this article can be found, in the online version, at doi:https://doi.org/10.1016/j.ijggc.2019.102952.

References

Aronu, U.E., Gondal, S., Hessen, E.T., Haug-Warberg, T., Hartono, A., Hoff, K.A., Svendsen, H.F., 2011. Solubility of CO_2 in 15, 30, 45 and 60 mass% MEA from 40 to 120°C and model representation using the extended UNIQUAC framework. Chem. Eng. Sci. 66, 6393–6406.

Aronu, U.E., Kim, I., Haugen, G., 2014. Evaluation of energetic benefit for solid-liquid phase change CO_2 absorbents. Energy Procedia 63, 532–541.

ASPEN, 2017. Aspen Technology Inc., Aspen Plus, v8.8 ed. AspenTech.

Barzagli, F., Giorgi, C., Mani, F., Peruzzini, M., 2018. Reversible carbon dioxide capture by aqueous and non-aqueous amine-based absorbents: a comparative analysis carried out by 13C NMR spectroscopy. Appl. Energy 220, 208–219.

Barzagli, F., Giorgi, C., Mani, F., Peruzzini, M., 2019. Comparative study of CO_2 capture by aqueous and nonaqueous 2-amino-2-methyl-1-propanol based absorbents carried out by 13C NMR and enthalpy analysis. Ind. Eng. Chem. Res. 58, 4364–4373.

Barzagli, F., Lai, S., Mani, F., Stoppioni, P., 2014. Novel non-aqueous amine solvents for biogas upgrading. Energy Fuels 28, 5252–5258.

Barzagli, F., Mani, F., Peruzzini, M., 2013. Efficient CO_2 absorption and low temperature desorption with non-aqueous solvents based on 2-amino-2-methyl-1-propanol (AMP). Int. J. Greenh. Gas Control. 16, 217–223.

Barzagli, F., Mani, F., Peruzzini, M., 2017. Novel water-free biphasic absorbents for efficient CO_2 capture. Int. J. Greenh. Gas Control. 60, 100–109.

Garcia, M., Knuutila, H.K., Aronu, U.E., Gu, S., 2018. Influence of substitution of water by organic solvents in amine solutions on absorption of CO_2. Int. J. Greenh. Gas Control. 78, 286–305.

Jou, F.-Y., Mather, A.E., Otto, F.D., 1995. The solubility of CO_2 in a 30 mass percent monoethanolamine solution. Can. J. Chem. Eng. 73, 140–147.

Karlsson, H., Svensson, H., 2018. Physical properties of the 2-amino-2-methyl-1-propanol and N-methyl-2-pyrrolidone system. SSRN.

Karlsson, H.K., Drabo, P., Svensson, H., 2019. Precipitating non-aqueous amine systems for absorption of carbon dioxide using 2-amino-2-methyl-1-propanol. Int. J. Greenh. Gas Control. 88, 460–468.

Kassim, D.M., Zainel, H.A., Al-Asaf, S.A., Talib, E.K., 1988. The temperature dependence of the solubility of carbon dioxide in several extraction solvents. Fluid Phase Equilib. 41, 287–294.

Kim, I., Hoff, K.A., Mejdell, T., 2014. Heat of absorption of CO_2 with aqueous solutions of MEA: new experimental data. Energy Procedia 63, 1446–1455.

Kim, I., Svendsen, H.F., 2007. Heat of Absorption of Carbon Dioxide (CO_2) in Monoethanolamine (MEA) and 2-(Aminoethyl)ethanolamine (AEEA) Solutions. pp. 5803–5809.

Knuutila, H.K., Nannestad, Å., 2017. Effect of the concentration of MAPA on the heat of absorption of CO_2 and on the cyclic capacity in DEEA-MAPA blends. Int. J. Greenh. Gas Control. 61, 94–103.

Liu, H., Chan, C., Tontiwachwuthikul, P., Idem, R., 2019a. Analysis of CO_2 equilibrium solubility of seven tertiary amine solvents using thermodynamic and ANN models. Fuel 249, 61–72.

Liu, H., Idem, R., Tontiwachwuthikul, P., 2019b. Novel models for correlation of Solubility constant and diffusivity of N_2O in aqueous 1-dimethylamino-2-propanol. Chem. Eng. Sci. 203, 86–103.

Ma'mun, S., Nilsen, R., Svendsen, H.F., Juliussen, O., 2005. Solubility of carbon dioxide in 30 mass % monoethanolamine and 50 mass % methyldiethanolamine solutions. J. Chem. Eng. Data 50, 630–634.

Meldon, J.H., 2011. Amine screening for flue gas CO_2 capture at coal-fired power plants: should the heat of desorption be high, low or in between? Curr. Opin. Chem. Eng. 1, 55–63.

Melzer, W.M., Schrödter, F., Knapp, H., 1989. Solubilities of methane, propane and carbon dioxide in solvent mixtures consisting of water, N,N-dimethylformamide, and N-methyl-2-pyrrolidone. Fluid Phase Equilib. 49, 167–186.

Mobley, P.D., Rayer, A.V., Tanthana, J., Gohndrone, T.R., Soukri, M., Coleman, L.J.I., Lail, M., 2017. CO_2 capture using fluorinated hydrophobic solvents. Ind. Eng. Chem. Res. 56, 11958–11966.

Murrieta-Guevara, F., Romero-Martinez, A., Trejo, A., 1988. Solubilities of carbon dioxide and hydrogen sulfide in propylene carbonate, N-methylpyrrolidone and sulfolane. Fluid Phase Equilib. 44, 105–115.

Murrieta-Guevara, F., Trejo Rodriguez, A., 1984. Solubility of carbon dioxide, hydrogen sulfide, and methane in pure and mixed solvents. J. Chem. Eng. Data 29, 456–460.

Pakzad, P., Mofarahi, M., Izadpanah, A.A., Afkhamipour, M., Lee, C.-H., 2018. An experimental and modeling study of CO_2 solubility in a 2-amino-2-methyl-1-propanol (AMP) + N-methyl-2-pyrrolidone (NMP) solution. Chem. Eng. Sci. 175, 365–376.

Rivas, O.R., Prausnitz, J.M., 1979. Sweetening of sour natural gases by mixed-solvent absorption: solubilities of ethane, carbon dioxide, and hydrogen sulfide in mixtures of physical and chemical solvents. Aiche J. 25, 975–984.

Sciamanna, S.F., Lynn, S., 1988. Solubility of hydrogen sulfide, sulfur dioxide, carbon dioxide, propane, and n-Butane in poly(glycol ethers). Ind. Eng. Chem. Res. 27, 492–499.

Shen, K.P., Li, M.H., 1992. Solubility of carbon dioxide in aqueous mixtures of monoethanolamine with methyldiethanolamine. J. Chem. Eng. Data 37, 96–100.

Sweeney, C.W.J.C., 1984. Solubilities and partial molar enthalpies of solution for polar gas-liquid systems determined by gas chromatography. Chromatographia 18, 663–667.

Svensson, H., Edfeldt, J., Zejnullahu Velasco, V., Hulteberg, C., Karlsson, H.T., 2014a. Solubility of carbon dioxide in mixtures of 2-amino-2-methyl-1-propanol and organic solvents. Int. J. Greenh. Gas Control. 27, 247–254.

Svensson, H., Hulteberg, C., Karlsson, H.T., 2014b. Precipitation of AMP carbamate in CO_2 absorption process. Energy Procedia 750–757.

Svensson, H., Karlsson, H., 2018. Solubility of carbon dioxide in mixtures of 2-amino-2-methyl-1-propanol and N-methyl-2-pyrrolidone at absorption and desorption conditions. SSRN.

Svensson, H., Zejnullahu Velasco, V., Hulteberg, C., Karlsson, H.T., 2014c. Heat of absorption of carbon dioxide in mixtures of 2-amino-2-methyl-1-propanol and organic solvents. Int. J. Greenh. Gas Control. 30, 1–8.

Tong, D., Trusler, J.P.M., Maitland, G.C., Gibbins, J., Fennell, P.S., 2012. Solubility of carbon dioxide in aqueous solution of monoethanolamine or 2-amino-2-methyl-1-propanol: experimental measurements and modelling. Int. J. Greenh. Gas Control. 6, 37–47.

Ye, Q., Wang, X., Lu, Y., 2015. Screening and evaluation of novel biphasic solvents for energy-efficient post-combustion CO_2 capture. Int. J. Greenh. Gas Control. 39, 205–214.

Yuan, Y., Rochelle, G.T., 2018. CO_2 absorption rate in semi-aqueous monoethanolamine. Chem. Eng. Sci. 182, 56–66.

Zhang, S., Shen, Y., Wang, L., Chen, J., Lu, Y., 2019. Phase change solvents for post-combustion CO_2 capture: principle, advances, and challenges. Appl. Energy 239, 876–897.

Zheng, C., Tan, J., Wang, Y.J., Luo, G.S., 2012. CO_2 solubility in a mixture absorption system of 2-amino-2-methyl-1-propanol with glycol. Ind. Eng. Chem. Res. 51, 11236–11244.

Zheng, C., Tan, J., Wang, Y.J., Luo, G.S., 2013. CO_2 solubility in a mixture absorption system of 2-amino-2-methyl-1-propanol with ethylene glycol. Ind. Eng. Chem. Res. 52, 12247–12252.

Zhou, X., Liu, F., Lv, B., Zhou, Z., Jing, G., 2017. Evaluation of the novel biphasic solvents for CO_2 capture: performance and mechanism. Int. J. Greenh. Gas Control. 60, 120–128.